Contents

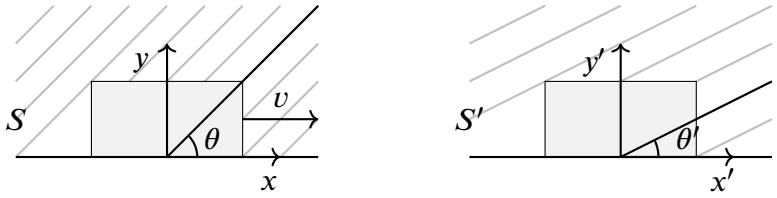

Figure 1: Path of the rain drops in a frame fixed to the ground and the train.

1 Aberration Formulas

1.1 Classical and Relativistic Aberration

Consider a train cart fixed to the frame S' moving in $+x$-direction with velocity v w.r.t. frame S fixed to the ground. Passenger on the train observes the direction of rain drops from the window. Suppose in S it is raining from direction θ w.r.t. the positive x axis. Then, the path of rain drop falling through $x = y = 0$ can be written

$$x(t) = -u\cos\theta\, t, \tag{1}$$
$$y(t) = -u\sin\theta\, t, \tag{2}$$

where u is the velocity of the rain drop in S. In S', we can express

$$x'(t) = -(u\cos\theta + v)t, \tag{3}$$
$$y'(t) = -u(\sin\theta)t. \tag{4}$$

In S', the angle θ' made by the rain drops w.r.t. positive x axis can be expressed

$$\tan\theta' = \frac{y'}{x'} = \frac{u\sin\theta}{u\cos\theta + v} = \frac{\tan\theta}{1+\beta\sec\theta}, \tag{5}$$

where $\beta = v/u$ and $\sec\theta = 1/\cos\theta$. This classical formula is limited angles in $+x$ direction. More generally,

$$\theta' = \operatorname{atan2}(\sin\theta, \cos\theta + \beta) \tag{6}$$

Consider now light in the context of Special Relativity with velocity vector $\boldsymbol{c} = (-c\cos\theta, -c\sin\theta, 0)$. Then, simple application of Lorentz transformation, yields

$$x' = \gamma(x - vt) = -\gamma(c\cos\theta + v)t, \tag{7}$$
$$y' = y = -(c\sin\theta)t, \tag{8}$$

where the **Lorentz factor** is defined

$$\gamma := \frac{1}{\sqrt{1 - v^2/c^2}} = \frac{1}{\sqrt{1-\beta^2}}. \tag{9}$$

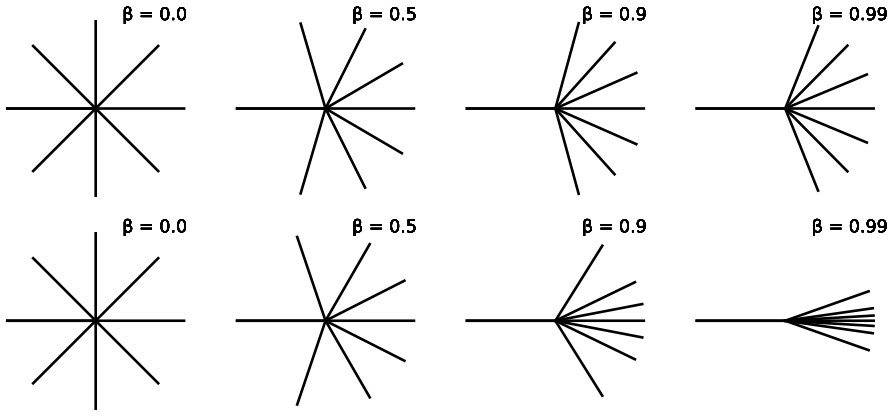

Figure 2: Difference between classical (top) and relativistic (bottom) aberration.

Thus, we obtain the well-known formula for relativistic aberration

$$\tan\theta' = \frac{y'}{x'} = \frac{\tan\theta}{\gamma(1+\beta\sec\theta)} \tag{10}$$

and the more general expression

$$\theta' = \operatorname{atan2}\left[\sin\theta, \gamma(\cos\theta+\beta)\right] \tag{11}$$

The only difference between classical and relativistic aberration is the Lorentz factor. When β is small, the difference between relativistic and classical results can be usually ignored. At velocities close to the speed of light, the Lorentz factor leads to light sources accumulating around direction of motion (see Figure 2).

1.2 General Vector Expression for Aberration

For practical computations, it is often more convenient to use vectors. Any vector expression for aberration will involve addition of velocity vectors, which is non-trivial in relativistic case.

1.2.1 Classical Aberration

In the classical case, the transformation of velocities is simply

$$\boldsymbol{u}' = \boldsymbol{u} - \boldsymbol{v}. \tag{12}$$

The direction to target $\hat{\mathbf{s}} = -\boldsymbol{u}'/|\hat{\mathbf{u}}'|$ corrected for aberration is called the **proper direction**. Unlike the relativistic expression $\hat{\mathbf{s}} = -\boldsymbol{u}'/c$, the classical expression for the proper direction needs to take into account that classical addition of velocities can lead to velocity of light greater than c. The **uncorrected direction** in both cases can be written $\hat{\mathbf{p}} = -\hat{\mathbf{u}}/c$.

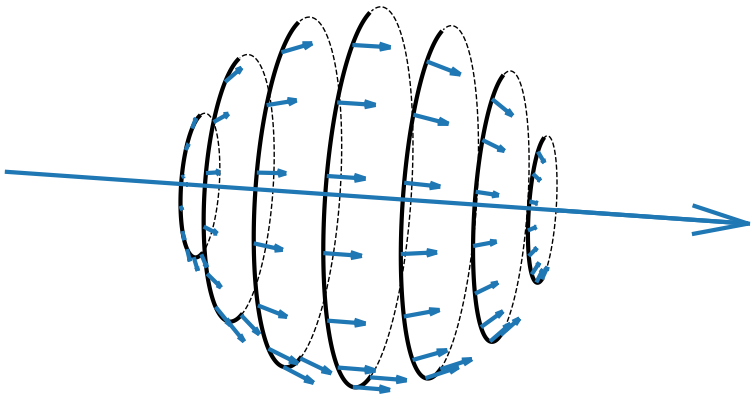

Figure 3: Three-dimensional depiction of the aberration correction for a velocity vector and the associated rotational symmetry.

Direct substitution to (12), yields

$$-\hat{\mathbf{s}}|c\hat{\mathbf{p}} + \boldsymbol{v}| = -c\hat{\mathbf{p}} - \boldsymbol{v} \tag{13}$$

and denoting $\boldsymbol{\beta} = \boldsymbol{v}/c$, we obtain the classical vector expression for proper direction

$$\boxed{\hat{\mathbf{s}} = \frac{\hat{\mathbf{p}} + \boldsymbol{v}/c}{|\hat{\mathbf{p}} + \boldsymbol{v}/c|} = \frac{\hat{\mathbf{p}} + \boldsymbol{\beta}}{|\hat{\mathbf{p}} + \boldsymbol{\beta}|}}. \tag{14}$$

1.2.2 General Lorentz Transformation of Velocities

Let S' move w.r.t. S with velocity $\boldsymbol{v}$ and denote

$$\boldsymbol{u} := \frac{d\boldsymbol{r}}{dt}, \quad \boldsymbol{u}' := \frac{d\boldsymbol{r}'}{dt'}, . \tag{15}$$

Then, the Lorentz transformation will only affect coordinates along the direction of the velocity. That is, parallel and perpendicular components of $d\boldsymbol{r}$ transform as

$$d\boldsymbol{r}'_{||} = \gamma\left(d\boldsymbol{r}_{||} - \boldsymbol{v}\, dt\right) \tag{16}$$

$$d\boldsymbol{r}'_{\perp} = d\boldsymbol{r}_{\perp}. \tag{17}$$

The time transforms as

$$dt' = \gamma\left(dt - \frac{\boldsymbol{v}\cdot d\boldsymbol{r}}{c^2}\right) = \gamma\left(1 - \frac{\boldsymbol{v}\cdot\boldsymbol{u}}{c^2}\right) dt. \tag{18}$$

Now we can expand the components of velocity in S'

$$\boldsymbol{u}'_{||} = \frac{d\boldsymbol{r}'_{||}}{dt'} = \frac{\gamma(\boldsymbol{r}_{||} - \boldsymbol{v}\, dt)}{\gamma(1 - \boldsymbol{v}\cdot\boldsymbol{u}/c^2)dt} = \frac{\boldsymbol{u}_{||} - \boldsymbol{v}}{1 - \boldsymbol{v}\cdot\boldsymbol{u}/c^2} \tag{19}$$

$$\boldsymbol{u}'_{\perp} = \frac{d\boldsymbol{r}'_{\perp}}{dt'} = \frac{d\boldsymbol{r}_{\perp}}{\gamma(1 - \boldsymbol{v}\cdot\boldsymbol{u}/c^2)dt} = \frac{\boldsymbol{u}_{\perp}}{\gamma(1 - \boldsymbol{v}\cdot\boldsymbol{u}/c^2)} \tag{20}$$

The velocity in S' can be expanded using

$$\boldsymbol{u}_{||} = \frac{\boldsymbol{u}\cdot\boldsymbol{v}}{v^2}\boldsymbol{v}, \quad \boldsymbol{u}_{\perp} = \boldsymbol{u} - \boldsymbol{u}_{||} = \boldsymbol{u} - \frac{\boldsymbol{u}\cdot\boldsymbol{v}}{v^2}\boldsymbol{v} \tag{21}$$

leading to

$$\begin{aligned}
\boldsymbol{u}' &= \boldsymbol{u}'_{||} + \boldsymbol{u}'_{\perp} && (22)\\
&= \frac{\boldsymbol{u}_{||} - \boldsymbol{v} + \boldsymbol{u}_{\perp}/\gamma}{1 - \boldsymbol{v}\cdot\boldsymbol{u}/c^2} && (23)\\
&= \frac{1}{1 - \boldsymbol{v}\cdot\boldsymbol{u}/c^2}\left[\frac{\boldsymbol{u}\cdot\boldsymbol{v}}{v^2}\boldsymbol{v} - \boldsymbol{v} + \frac{1}{\gamma}\left(\boldsymbol{u} - \frac{\boldsymbol{u}\cdot\boldsymbol{v}}{v^2}\boldsymbol{v}\right)\right] && (24)\\
&= \frac{1}{1 - \boldsymbol{v}\cdot\boldsymbol{u}/c^2}\left\{\frac{1}{\gamma}\boldsymbol{u} + \boldsymbol{v}\left[\frac{\boldsymbol{u}\cdot\boldsymbol{v}}{v^2}\left(1 - \frac{1}{\gamma}\right) - 1\right]\right\} && (25)\\
&= \frac{1}{\gamma(1 - \boldsymbol{v}\cdot\boldsymbol{u}/c^2)}\left[\boldsymbol{u} + \boldsymbol{v}\left(\frac{\boldsymbol{u}\cdot\boldsymbol{v}}{v^2}(\gamma - 1) - \gamma\right)\right]. && (26)
\end{aligned}$$

1.2.3 Relativistic Aberration

Let $\hat{\mathbf{n}} = \boldsymbol{u}/c$ be the direction of light propagation and $\hat{\mathbf{s}} = -\boldsymbol{u}'/c$ be the (relativistic) proper direction. Substitution to the General Lorentz Transformation for velocities (26) then yields

$$-c\hat{\mathbf{s}} = \frac{1}{\gamma(1 - \hat{\mathbf{n}}\cdot\boldsymbol{v}/c)}\left\{c\hat{\mathbf{n}} + \boldsymbol{v}\left[\frac{c}{v^2}(\hat{\mathbf{n}}\cdot\boldsymbol{v})(\gamma - 1) - \gamma\right]\right\} \tag{27}$$

or

$$\begin{aligned}
\hat{\mathbf{s}} &= \frac{1}{\gamma(1 - \hat{\mathbf{n}}\cdot\boldsymbol{v}/c)}\left\{-\hat{\mathbf{n}} + \boldsymbol{v}\left[\frac{\gamma}{c} - \frac{1}{v^2}(\hat{\mathbf{n}}\cdot\boldsymbol{v})(\gamma - 1)\right]\right\} && (28)\\
&= \frac{1}{\gamma(1 - \hat{\mathbf{n}}\cdot\boldsymbol{v}/c)}\left\{-\hat{\mathbf{n}} + \boldsymbol{v}\frac{\gamma}{c}\left[1 - \frac{c}{v^2}(\hat{\mathbf{n}}\cdot\boldsymbol{v})\frac{\gamma - 1}{\gamma}\right]\right\} && (29)\\
&= \frac{1}{\gamma(1 - \hat{\mathbf{n}}\cdot\boldsymbol{v}/c)}\left[-\hat{\mathbf{n}} + \boldsymbol{v}\frac{\gamma}{c}\left(1 - \frac{\gamma}{\gamma + 1}\frac{\boldsymbol{v}\cdot\hat{\mathbf{n}}}{c}\right)\right], && (30)
\end{aligned}$$

where in the last step we have used

$$\begin{aligned}
\frac{\gamma - 1}{\gamma\beta^2} &= \frac{\gamma - 1}{\gamma(1 - \gamma^{-2})} = \frac{\gamma^2 - \gamma}{\gamma^2 - 1} = \gamma\frac{\gamma - 1}{(\gamma - 1)(\gamma + 1)} = \frac{\gamma}{\gamma + 1} && (31)\\
\Rightarrow \frac{c}{v^2}\frac{\gamma - 1}{\gamma}(\boldsymbol{v}\cdot\hat{\mathbf{n}}) &= \frac{1}{c}\frac{\gamma - 1}{\gamma\beta^2}(\boldsymbol{v}\cdot\hat{\mathbf{n}}) && (32)
\end{aligned}$$

Denoting $\boldsymbol{\beta} = \boldsymbol{v}/c$, we obtain expression for the proper direction

$$\hat{\mathbf{s}} = \frac{1}{\gamma(1 - \hat{\mathbf{n}}\cdot\boldsymbol{\beta})}\left[-\hat{\mathbf{n}} + \gamma\boldsymbol{\beta}\left(1 - \frac{\gamma}{\gamma + 1}\boldsymbol{\beta}\cdot\hat{\mathbf{n}}\right)\right] \tag{33}$$

Let $\boldsymbol{p} = -\hat{\mathbf{n}}$ be the uncorrected direction. Then (33) can be expressed

$$\boxed{\hat{\mathbf{s}} = \frac{1}{\gamma(1 + \hat{\mathbf{p}}\cdot\boldsymbol{\beta})}\left[\hat{\mathbf{p}} + \gamma\boldsymbol{\beta}\left(1 + \frac{\gamma}{\gamma + 1}\boldsymbol{\beta}\cdot\hat{\mathbf{p}}\right)\right].} \tag{34}$$

1.3 Series Expansion of Aberration Correction

1.3.1 Classical Aberration

Cross product of (14) with uncorrected direction $\boldsymbol{p}$, yields

$$\sin\Delta\theta\,\hat{\mathbf{n}} = \hat{\mathbf{p}}\times\hat{\mathbf{s}} = \frac{\hat{\mathbf{p}}\times\hat{\mathbf{p}}+\hat{\mathbf{p}}\times\boldsymbol{\beta}}{|\hat{\mathbf{p}}+\boldsymbol{\beta}|} = \frac{\hat{\mathbf{p}}\times\boldsymbol{\beta}}{|\hat{\mathbf{p}}+\boldsymbol{\beta}|} = \frac{||\hat{\mathbf{p}}||\,||\boldsymbol{\beta}||\sin\theta\,\hat{\mathbf{n}}}{|\hat{\mathbf{p}}+\boldsymbol{\beta}|} = \frac{\beta\sin\theta\,\hat{\mathbf{n}}}{\sqrt{1+2\beta\cos\theta+\beta^2}}, \quad (35)$$

where we have used

$$\begin{aligned} ||\hat{\mathbf{p}}+\boldsymbol{\beta}||^2 &= (||\hat{\mathbf{p}}|| + ||\boldsymbol{\beta}||\cos\theta)^2 + \beta^2\sin^2\theta & (36)\\ &= 1 + 2\beta\cos\theta + \beta^2\cos^2\theta + \beta^2\sin^2\theta & (37)\\ &= 1 + 2\beta\cos\theta + \beta^2. & (38)\end{aligned}$$

According to generalized binomial theorem

$$\frac{1}{\sqrt{1+x}} = \sum_{k=0}^{\infty}\binom{-1/2}{k}x^n \approx 1 - \frac{1}{2}x + \frac{3}{8}x^2 - \frac{5}{16}x^3 + ... \quad (39)$$

Substitution of $x = 2\beta\cos\theta+\beta^2$, yields

$$\begin{aligned} \frac{1}{\sqrt{1+2\beta\cos\theta+\beta^2}} &\approx 1 - \frac{1}{2}(2\beta\cos\theta+\beta^2) + \frac{3}{8}(2\beta\cos\theta+\beta^2)^2 & (40)\\ &= 1 - \cos\theta\beta + \left(\frac{3}{2}\cos^2\theta - \frac{1}{2}\right)\beta^2 + \frac{3}{2}\cos\theta\beta^3 + \frac{3}{8}\beta^4 & (41)\end{aligned}$$

and if we ignore everything above fourth power of β, we can expand

$$\sin\Delta\theta \approx \beta\sin\theta - \frac{1}{2}\beta^2\sin 2\theta + \frac{1}{8}\beta^3(3\sin 3\theta - \sin\theta) + \frac{3}{4}\beta^4\sin 2\theta \quad (42)$$

Note that when such a series is expressed as a linear combination of sinusoidal terms, it is obvious that $\Delta\theta$ antisymmetric w.r.t. θ and zero at $\theta = 0$. The above formula also produces a positive $\Delta\theta$ with positive θ, which is incorrect. In most applications, where β is small, we can approximate

$$\boxed{\Delta\theta \approx \sin\Delta\theta \approx -\beta\sin\theta + \frac{1}{2}\beta^2\sin 2\theta.} \quad (43)$$

1.3.2 Relativistic Aberration

Cross product of (34) with uncorrected direction $\hat{\mathbf{p}}$, yields

$$\begin{aligned} ||\hat{\mathbf{s}}||\,||\hat{\mathbf{p}}||\sin\Delta\theta\hat{\mathbf{n}} &= \hat{\mathbf{s}}\times\hat{\mathbf{p}} & (44)\\ &= \frac{\boldsymbol{\beta}\times\hat{\mathbf{p}}}{1+\hat{\mathbf{p}}\cdot\boldsymbol{\beta}}\left(1 + \frac{\gamma}{\gamma+1}\boldsymbol{\beta}\cdot\hat{\mathbf{p}}\right) & (45)\\ &= \frac{\beta\sin\theta}{1+\beta\cos\theta}\left(1 + \frac{\gamma}{\gamma+1}\beta\cos\theta\right)\hat{\mathbf{n}}. & (46)\end{aligned}$$

To obtain a series expansion for $\sin\Delta\theta$, note that:

$$\frac{1}{1+\beta\cos\theta} = \sum_{k=0}^{\infty}(-1)^k\beta^k\cos^k\theta \approx 1-\beta\cos\theta+\beta^2\cos^2\theta, \tag{47}$$

$$\frac{\gamma}{\gamma+1} = \frac{1}{1+\sqrt{1-\beta^2}} = \frac{1}{1+\sqrt{1-\beta^2}}\frac{1-\sqrt{1-\beta^2}}{1-\sqrt{1-\beta^2}} = \frac{1-\sqrt{1-\beta^2}}{\beta^2}, \tag{48}$$

$$\sqrt{1-\beta^2} = \sum_{k=0}^{\infty}\binom{1/2}{k}(-1)^k\beta^{2k} \approx 1-\frac{1}{2}\beta^2+\frac{1}{8}\beta^4. \tag{49}$$

Thus, we can also expand

$$\frac{1-\sqrt{1-\beta^2}}{\beta^2} \approx \frac{1}{\beta^2}\left[1-\left(1-\frac{1}{2}\beta^2+\frac{1}{8}\beta^4\right)\right] = \frac{1}{2}-\frac{1}{8}\beta^2, \tag{50}$$

$$\beta\sin\theta\left(1+\frac{\gamma}{\gamma+1}\beta\cos\theta\right) \approx \beta\sin\theta+\beta^2\sin\theta\cos\theta\left(\frac{1}{2}-\frac{1}{8}\beta^2\right) \approx \beta\sin\theta+\frac{1}{4}\beta^2\sin 2\theta \tag{51}$$

and finally

$$\sin\Delta\theta \approx (1-\beta\cos\theta)\left(\beta\sin\theta+\frac{1}{4}\beta^2\sin 2\theta\right) \tag{52}$$

$$\approx \beta\sin\theta-\beta^2\sin\theta\cos\theta+\frac{1}{4}\beta^2\sin 2\theta \tag{53}$$

Thus, again noting the sign, we obtain the approximation

$$\boxed{\Delta\theta \approx \sin\Delta\theta \approx -\beta\sin\theta+\frac{1}{4}\beta^2\sin 2\theta.} \tag{54}$$

1.3.3 Accuracy

The difference in the quadratic term between (54) and (43) suggests that the linear approximation can be more preferrable than the quadratic classical approximation. Comparison with two values of θ is shown in Figure 4. Worst case (w.r.t. θ) relative errors are shown in Figure 5.

The linear approximation is usually sufficient for most purposes in astrometry: For example, if Earth's speed along it's orbit is about 30 km/s or $\beta \approx 10^{-4}$, the maximum relative error from linear and quadratic approximations are on the scale of 10^{-4} and 10^{-8}, respectively. If the maximum aberration is around 20", this corresponds to absolute errors around 2 mas and 0.2 μas, respectively.

1.4 Spherical Coordinates

We expand uncorrected direction

$$\hat{\mathbf{p}} = \begin{bmatrix}\cos\delta\cos\alpha\\ \cos\delta\sin\alpha\\ \sin\delta\end{bmatrix}, \tag{55}$$

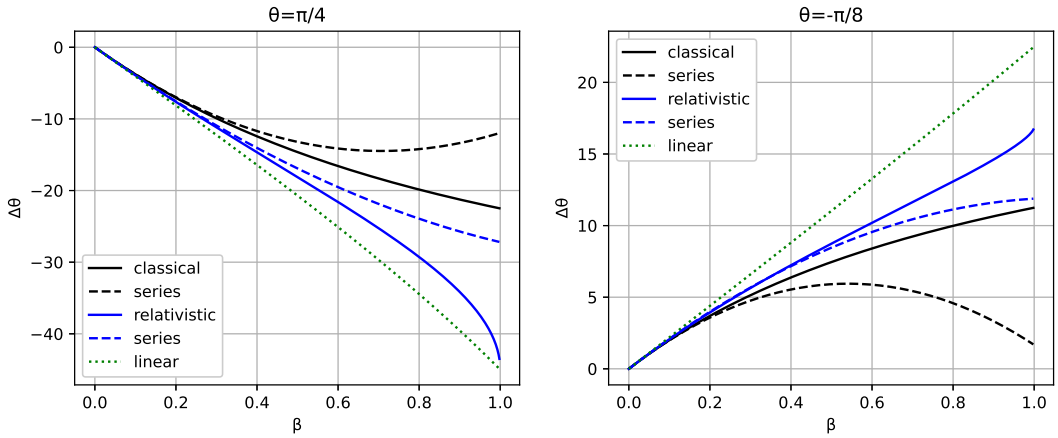

Figure 4: Linear and quadratic approximation of classical and relativistic aberration.

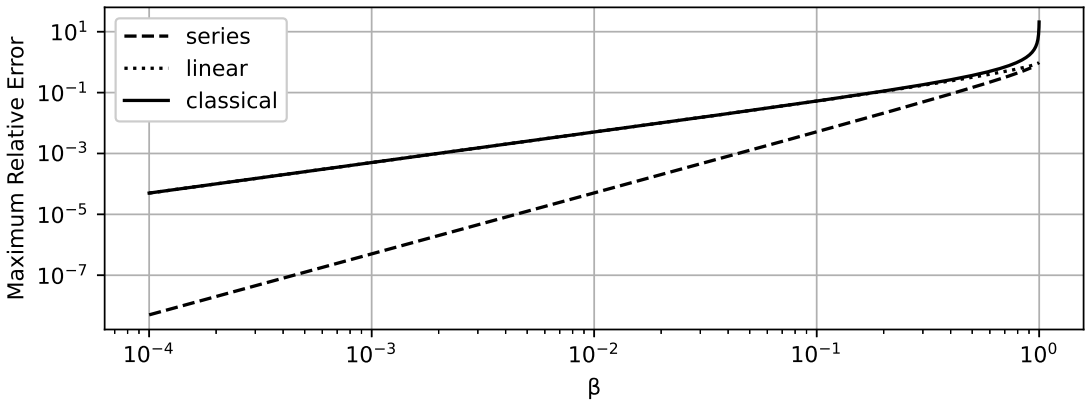

Figure 5: Maximum aberration error with respect to the exact relativistic formula.

where δ and α are the declination and the right ascension, respectively (in appropriate frames). Then, unit vectors along the declination and right ascension coordinates can be written

$$\hat{\mathbf{e}}_\delta = \frac{\partial \hat{\mathbf{p}}}{\partial \delta} = \begin{bmatrix} -\sin\delta\cos\alpha \\ -\sin\delta\sin\alpha \\ \cos\delta \end{bmatrix}, \quad \hat{\mathbf{e}}_\alpha = \frac{1}{\cos\delta}\frac{\partial \hat{\mathbf{p}}}{\partial \alpha} = \begin{bmatrix} -\sin\alpha \\ \cos\alpha \\ 0 \end{bmatrix}. \tag{56}$$

Thus, for small $\hat{\mathbf{s}} - \hat{\mathbf{p}}$, we can approximate

$$\Delta\delta = (\hat{\mathbf{s}} - \hat{\mathbf{p}}) \cdot \hat{\mathbf{e}}_\delta \tag{57}$$
$$\cos\delta\Delta\alpha = (\hat{\mathbf{s}} - \hat{\mathbf{p}}) \cdot \hat{\mathbf{e}}_\alpha \tag{58}$$

For small v/c, we can approximate from (14)

$$\hat{\mathbf{s}} - \hat{\mathbf{p}} \approx \boldsymbol{\beta}. \tag{59}$$

Thereafter, we obtain

$$\Delta\delta = \hat{\mathbf{e}}_\delta \cdot \boldsymbol{\beta} = -\beta_x \sin\delta\cos\alpha - \beta_y \sin\delta\sin\alpha + \beta_z\cos\delta \tag{60}$$
$$\cos\delta\Delta\alpha = \hat{\mathbf{e}}_\alpha \cdot \boldsymbol{\beta} = -\beta_x\sin\alpha + \beta_y\cos\alpha. \tag{61}$$

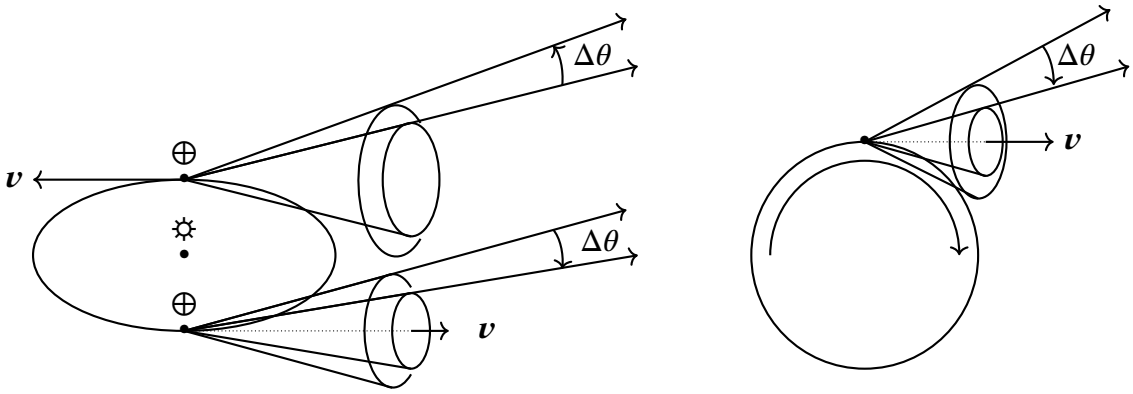

Figure 6: Annual aberration correction for a planet orbiting the Sun (left). Diurnal aberration correction for an observer on the surface of a rotating planet (right). The cones depict rotational symmetry in the correction.

2 Stellar Aberration

Stellar aberration refers to the apparent change in the position of a stellar object due to velocity of the observer. For an observer fixed to the surface of a rotating planet, the stellar aberration may involve:

- **Annual aberration** resulting from the motion of the planet around the barycenter of the solar system. For Earth, the velocity of 29.79 km/s around the barycenter of the solar system amounts to a maximum correction on 20.496 arcseconds.
- **Diurnal aberration** resulting from the rotation of the planet. At the equator, Earth rotates approximately with the tangential velocity of 465 meters per second, which amounts to a maximum correction of 0.32 arcseconds.
- **Secular aberration** resulting from the approximately unifrom motion of the solar system around the center of the galaxy. For our solar system, this velocity. is about 220 km/s and amounts to a maximum correction of 150". However, since the velocity changes very slowly, the effect is included in the catalogued positions and is not corrected.
- **Planetary aberration** resulting from both the motion of the observer and the movement of the observed body.

Aberration can also result from the observer moving w.r.t. the surface of the planet. For example, a fighter jet or a missile can travel at speeds higher than the rotation speed of Earth. However, this effect is likely always small enough to be neglected in technical applications. For a satellite on LEO moving at 8 km/s w.r.t. inertial frame centered on Earth, the maximum aberration is around 5.5 arcseconds.

The expressions developed in the previous section apply to all types of aberration.

2.1 Linear Approximation in Spherical Coordinates

2.1.1 Annual Aberration

For elliptic orbits, the velocity and distance from the center can be expressed

$$v = \sqrt{\mu\left(\frac{2}{r} - \frac{1}{a}\right)}, \quad r = \frac{a(1-e^2)}{1 + e\cos f}. \tag{62}$$

At perihelion and aphelion $f = 0$ and $f = 180°$, respectively corresponding to maximum and minimum velocities

$$v_{max} = \sqrt{\frac{\mu}{a}\left(\frac{1+e}{1-e}\right)}, \quad v_{min} = \sqrt{\frac{\mu}{a}\left(\frac{1-e}{1+e}\right)}. \tag{63}$$

For Earth's orbit around the Sun, we can substitue $\mu = 1.32712440042 \cdot 10^{20}\,\mathrm{m^3 s^{-2}}$, $e = 0.01671022$ and $a = 1.495980229607128 \cdot 10^{11}$ m leading to

$$v_{max} = 30286.614 \text{ m/s}, \quad v_{min} = 29291.058 \text{ m/s}, \quad v_{avg} = 29790.915 \text{ m/s}. \tag{64}$$

The **constant of aberration** κ is the maximum possible displacement of a distant object due to aberration and can be approximated $\kappa \approx v/c$. Correspondingly, we obtain

$$\kappa_{max} = 20.838'', \quad \kappa_{min} = 20.153'', \quad \kappa_{avg} = 20.497''. \tag{65}$$

To obtain geometric intuition about annual aberration throughout the year, consider a circular orbit with zero inclination. That is,

$$\boldsymbol{\beta}(t) \;=\; \beta(\cos\omega t, \sin\omega t, 0). \tag{66}$$

Substitution to (60) and (61), yields

$$\begin{aligned} \Delta\delta &= -\beta\sin\delta\cos\alpha\cos\omega t - \beta\sin\delta\sin\alpha\sin\omega t & (67)\\ \cos\delta\Delta\alpha &= -\beta\sin\alpha\cos\omega t + \beta\cos\alpha\sin\omega t. & (68) \end{aligned}$$

Suppose $\alpha = 0$. Then, the above simplifies to

$$\begin{aligned} \Delta\delta &= -\beta\sin\delta\cos\omega t, & (69)\\ \cos\delta\Delta\alpha &= \beta\sin\omega t. & (70) \end{aligned}$$

That is, annual aberration will lead to a displacement shaped like an ellipse with a period of one orbit (see Figure 7).

2.1.2 Diurnal Aberration

The velocity of the observer on the surface of Earth can be written

$$v = \omega(R + h)\cos\phi, \tag{71}$$

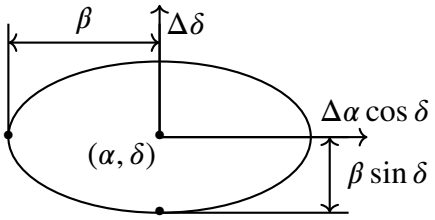

Figure 7: Elliptical shape of abberation correction w.r.t. the uncorrected position.

where R, h and ϕ are the radius of Earth, altitude of the observer above the surface of Earth and the latitude. Consequently, the aberration can be approximated

$$\Delta\theta \approx \beta \approx \frac{\omega(R+h)}{c}\cos\phi. \tag{72}$$

Substitution of $R = 6371$ km, $\omega = 2\pi/86164.0905$ s yields at the equator

$$\Delta\theta \approx -0.3196''. \tag{73}$$

The velocity is always approximately towards the east corresponding to the x-axis in the ENU frame. That is, substituting $\boldsymbol{\beta} = \beta\hat{\mathbf{x}}$ to (60) and (61), yields

$$\begin{aligned} \Delta\delta &= -\beta\sin\delta\cos\alpha & (74)\\ \cos\delta\Delta\alpha &= -\beta\sin\alpha. & (75) \end{aligned}$$

The notation above is misleading in the sense δ and α do not refer to declination and right ascension. To obtain an expression in terms of elevation and azimuth, substitute for $a = \delta$ and $\alpha = 90° - \phi$ to obtain

$$\begin{aligned} \Delta a &= -\beta\sin a\sin\phi, & (76)\\ \cos a\Delta\phi &= \beta\cos\phi. & (77) \end{aligned}$$

For $\phi = 90°$ (east), we obtain $\Delta a = -\beta\sin a$ and for $a = 0$, we obtain $\Delta\phi = \beta\cos\phi = -\beta\sin(\phi - 90°)$, which is consistent with (54).

2.2 Planetary Aberration and Light-Time

The travel time of light between target and the observer is called **light-time** and denoted τ. When the direction to target changes significantly during light-time, this requires a correction. The relative apparent position to target can be expressed

$$\boldsymbol{p}(t) = \boldsymbol{u}_B(t-\tau) - \boldsymbol{E}_B(t), \tag{78}$$

where $\boldsymbol{u}_B$ and $\boldsymbol{E}_B$ are the barycentric positions of the target and the observer. Application of (14) yields

$$\begin{aligned} \boldsymbol{s}(t) &= \boldsymbol{p}(t) + \beta|\boldsymbol{p}| && (79)\\ &= \boldsymbol{u}_B(t-\tau) - \boldsymbol{E}_B(t) + \frac{|\boldsymbol{p}|}{c}\dot{\boldsymbol{E}}_B(t) && (80)\\ &= \boldsymbol{u}_B(t-\tau) - \boldsymbol{E}_B(t) + \tau\dot{\boldsymbol{E}}_B(t) && (81)\\ &\approx \boldsymbol{u}_B(t-\tau) - \boldsymbol{E}_B(t-\tau). && (82) \end{aligned}$$

That is, correcting for planetary aberration at t with classical approximation (14) is equivalent to the computation the uncorrected direction to target at $t-\tau$. Note that this does not take into account the diurnal aberration.

2.3 Practical Computation

The positions of stars are typically catalogued w.r.t. the Solar System Barycenter (SSB) so that secular aberration is already included in the catalogued positions. Thus, to compute the aberration correction for an observer, we need to compute the velcoity vector of the observer w.r.t. the SSB. For an observer on Earth, this velocity is the sum of the orbital velocity of the Earth around the SSB and the rotational velocity of the topocentric position of the observer around the geocenter (GEO) of Earth. Thereafter, (14) and (34) can be applied in any topocentric frame centered on the observer position.

2.3.1 Transformations Between Frames

Let us denote the position and velocity coordinate vector for target C in frame with orientation A and origin B with $\boldsymbol{r}^B_{C(A)}$ and $\boldsymbol{v}^B_{C(A)}$. Omission of C, A or B in an expression signifies that the expression applies for all targets, orientations or origins, respectively. Then, if R^a_A is the rotation matrix from orientation a to A, we can write

$$\boldsymbol{r}_{(A)} = R^a_A \boldsymbol{r}_{(a)} \quad \Leftrightarrow \quad \boldsymbol{r}^B_{C(A)} = R^a_A \boldsymbol{r}^B_{C(a)} \quad \forall B, C. \tag{83}$$

Similarly, for any two origins B and b

$$\boldsymbol{r}^B = \boldsymbol{r}^b - \boldsymbol{r}^b_B \quad \Leftrightarrow \quad \boldsymbol{r}^B_{C(A)} = \boldsymbol{r}^b_{C(A)} - \boldsymbol{r}^b_{B(A)} \quad \forall A, C. \tag{84}$$

The equation (83) does not apply to velocity vectors unless the rotation matrix is constant w.r.t. time. More generally, we can expand

$$\boldsymbol{v}_{(A)} = \frac{d}{dt}\boldsymbol{r}_{(A)} = \frac{d}{dt}\left(R^a_A \boldsymbol{r}_{(a)}\right) = \dot{R}^a_A \boldsymbol{r}_{(a)} + R^a_A \boldsymbol{v}_{(a)}, \tag{85}$$

where the $\dot{R}^a_A \boldsymbol{r}_{(a)}$ corresponds to velocity component from the rotation of $\boldsymbol{r}_{(a)}$ w.r.t. the origin.

2.3.2 Expansion of the Observer Velocity

The position and velocity vectors w.r.t. origins at the GEO and the SSB can be related by

$$\boldsymbol{r}^{GEO} = \boldsymbol{r}^{SSB} - \boldsymbol{r}^{SSB}_{GEO}, \tag{86}$$
$$\boldsymbol{v}^{GEO} = \boldsymbol{v}^{SSB} - \boldsymbol{v}^{SSB}_{GEO}, \tag{87}$$

where $\boldsymbol{v}^{SSB}_{GEO}$ is the orbital velocity of the geocenter w.r.t. the SSB. The rotation of the Earth can be expressed via the coordinate transform between inertial True-of-Date (ToD) and Pseudo-Earth-Fixed (PEF) frames

$$\boldsymbol{r}^{GEO}_{(PEF)} = R^{TOD}_{PEF}\boldsymbol{r}^{GEO}_{(TOD)} \quad : \quad R^{TOD}_{PEF} = \begin{bmatrix} \cos GAST & \sin GAST & 0 \\ -\sin GAST & \cos GAST & 0 \\ 0 & 0 & 1 \end{bmatrix}, \tag{88}$$

$$\boldsymbol{r}^{GEO}_{(TOD)} = R^{PEF}_{TOD}\boldsymbol{r}^{GEO}_{(PEF)} \quad : \quad R^{PEF}_{TOD} = \begin{bmatrix} \cos GAST & -\sin GAST & 0 \\ \sin GAST & \cos GAST & 0 \\ 0 & 0 & 1 \end{bmatrix}. \tag{89}$$

where GAST is the Greenwich Apparent Sidereal Time. The corresponding velocities can be expanded

$$\boldsymbol{v}^{GEO}_{(PEF)} = R^{TOD}_{PEF}\boldsymbol{v}^{GEO}_{(TOD)} + \dot{R}^{TOD}_{PEF}\boldsymbol{r}^{GEO}_{(TOD)}, \tag{90}$$
$$\boldsymbol{v}^{GEO}_{(TOD)} = R^{PEF}_{TOD}\boldsymbol{v}^{GEO}_{(PEF)} + \dot{R}^{PEF}_{TOD}\boldsymbol{r}^{GEO}_{(PEF)}, \tag{91}$$

where

$$\dot{R}^{TOD}_{PEF} = \frac{dGAST}{dt}\begin{bmatrix} -\sin GAST & \cos GAST & 0 \\ -\cos GAST & -\sin GAST & 0 \\ 0 & 0 & 0 \end{bmatrix} \tag{92}$$

$$\dot{R}^{PEF}_{TOD} = \frac{dGAST}{dt}\begin{bmatrix} -\sin GAST & -\cos GAST & 0 \\ \cos GAST & -\sin GAST & 0 \\ 0 & 0 & 0 \end{bmatrix}. \tag{93}$$

For computation of diurnal aberration amounting to less than 0.32 arcseconds, we can approximate the time derivative of GAST using the length of a sidereal day

$$\frac{dGAST}{dt} \approx \frac{2\pi \text{ rad}}{86164.0905\ s} \approx 7.2921159 \cdot 10^{-5}\text{rad/s} \approx 15.04107°/h. \tag{94}$$

The velocity of the observer w.r.t. the SSB can be expressed

$$\boldsymbol{v}^{SSB}_{(ECL)} = \boldsymbol{v}^{SSB}_{GEO,(ECL)} + R^{TOD}_{ECL}\boldsymbol{v}^{GEO}_{(TOD)} \tag{95}$$
$$= \boldsymbol{v}^{SSB}_{GEO,(ECL)} + R^{TOD}_{ECL}\left(R^{PEF}_{TOD}\boldsymbol{v}^{GEO}_{(PEF)} + \dot{R}^{PEF}_{TOD}\boldsymbol{r}^{GEO}_{(PEF)}\right). \tag{96}$$

The position of the observer $\boldsymbol{r}^{GEO}_{(PEF)} = R^{EFI}_{PEF}\boldsymbol{r}^{GEO}_{(EFI)}$, where $\boldsymbol{r}^{GEO}_{(EFI)}$ can obtained from geodetic position on WGS84. For an observer that is stationary w.r.t. surface of Earth $\boldsymbol{v}^{GEO}_{(PEF)} = \boldsymbol{0}$.

Aberration corrections (14) and (34) can be applied in the ecliptic frame centered on the SSB or the topocentric ENU frame of the observer. Application in an ENU frame requires rotation

$$\boldsymbol{R}_{ENU}^{ECL}\boldsymbol{v}_{(ECL)}^{SSB} = \boldsymbol{R}_{ENU}^{ECL}\boldsymbol{v}_{GEO,(ECL)}^{SSB} + \boldsymbol{R}_{ENU}^{TOD}\left(\boldsymbol{R}_{TOD}^{PEF}\boldsymbol{v}_{(PEF)}^{GEO} + \dot{\boldsymbol{R}}_{TOD}^{PEF}\boldsymbol{r}_{(PEF)}^{GEO}\right). \tag{97}$$

Note that since the aberration relates to the velocity difference between the observer and the SSB in an inertial frame, it is not appropriate to transfer the velocity of SSB to a topocentric frame, where it would rotate around the observer location at very high speed.

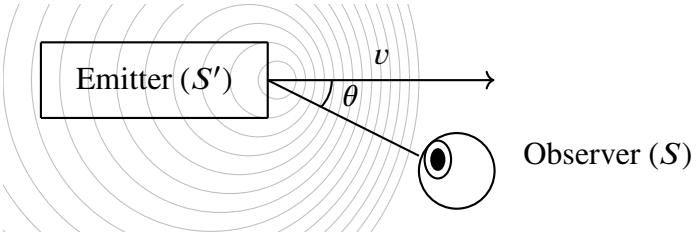

Figure 8: Geometry associated to Doppler Effect.

3 Doppler Effect

3.1 Classical and Relativistic Doppler Effect

Consider a light source fixed to an inertial frame S' moving with velocity v w.r.t. an observer fixed to an inertial frame S (see Figure 8). Suppose that the direction of movement makes the angle θ w.r.t. direction to the observer. Let $\boldsymbol{v} = v\hat{\mathbf{x}}$ and represent the wavefront towards the observer with phase angle

$$\phi(\boldsymbol{x}, t) = A\cos(\boldsymbol{k}\cdot\boldsymbol{x} - \omega t), \tag{98}$$

where the wave vector satisfies

$$\boldsymbol{k} = k\cos\theta\,\hat{\mathbf{x}} + k\sin\theta\,\hat{\mathbf{y}}. \tag{99}$$

Substitution of $kx - \omega t = 0$ yields in vacuum $x = \omega t/k = ct$ and $k = \omega/c$.

The phase angle ϕ in the frames S and S' can be related by the Galilean transformation

$$\begin{aligned} t &= t' && (100)\\ x &= x' + vt && (101)\\ y &= y' && (102)\\ z &= z' && (103) \end{aligned}$$

with the expansion

$$\begin{aligned} \boldsymbol{k}\cdot\boldsymbol{x} - \omega t &= kx\cos\theta + ky\sin\theta - \omega t && (104)\\ &= k(x' + vt)\cos\theta + ky\sin\theta - \omega t && (105)\\ &= kx'\cos\theta + ky'\sin\theta - \omega(1 - \beta\cos\theta) && (106)\\ &= \boldsymbol{k}'\cdot\boldsymbol{x}' - \omega' t && (107) \end{aligned}$$

Thus, we obtain the expression for **classical Doppler Effect**

$$\boxed{\omega = \frac{\omega'}{1 - \beta\cos\theta}, \quad \boldsymbol{k}' = \boldsymbol{k}.} \tag{108}$$

In the relativistic case, we replace the Galilean transformation with the Lorentz transformation

$$t = \gamma(t' + \beta x'/c) \tag{109}$$
$$x = \gamma(x' + vt) \tag{110}$$
$$y = y' \tag{111}$$
$$z = z'. \tag{112}$$

Now we can expand

$$\begin{aligned} \boldsymbol{k}\cdot\boldsymbol{x} - \omega t &= k\gamma(x' + vt')\cos\theta + ky\sin\theta - \omega\gamma(t' + \beta x'/c) && (113)\\ &= \gamma(k\cos\theta - \omega\beta/c)x' + ky\sin\theta - \gamma(\omega - kv\cos\theta))t' && (114)\\ &= \gamma k(\cos\theta - \beta)x' + ky'\sin\theta - \gamma\omega(1 - \beta\cos\theta)t' && (115)\\ &= \boldsymbol{k}'\cdot\boldsymbol{x}' - \omega' t' && (116) \end{aligned}$$

and obtain the expression for **relativistic Doppler Effect**

$$\boxed{\omega = \frac{\omega'}{\gamma(1 - \beta\cos\theta)}, \quad \boldsymbol{k}' = \gamma k(\cos\theta - \beta)\hat{\mathbf{x}} + k\sin\theta\hat{\mathbf{y}}.} \tag{117}$$

The transformation of the wave vector corresponds to the relativistic aberration correction.

3.2 Interpretation

3.2.1 Longitudal Doppler Effect

The special cases relating to longitudal motion are depicted in Figure 9. When $\theta = 180°$ and $\theta = 0°$, we can expand

$$\frac{\omega}{\omega'} = \frac{1}{\gamma(1+\beta)} = \frac{\sqrt{(1+\beta)(1-\beta)}}{1+\beta} = \sqrt{\frac{1-\beta}{1+\beta}} \leq 1 \tag{118}$$

$$\frac{\omega}{\omega'} = \frac{1}{\gamma(1-\beta)} = \frac{\sqrt{(1+\beta)(1-\beta)}}{1-\beta} = \sqrt{\frac{1+\beta}{1-\beta}} \geq 1 \tag{119}$$

respectively.

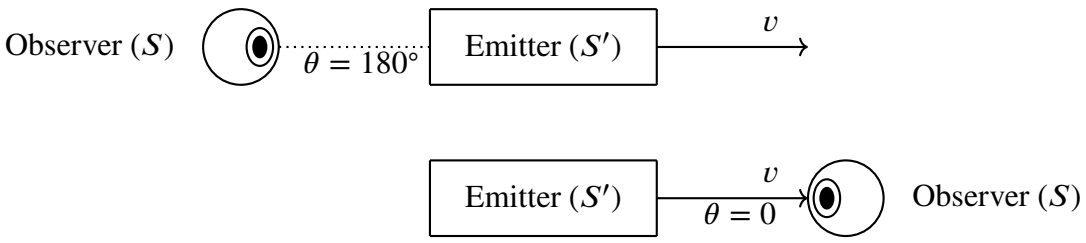

Figure 9: Geometry associated to maximal redshift (top) and maximal blueshift (below).

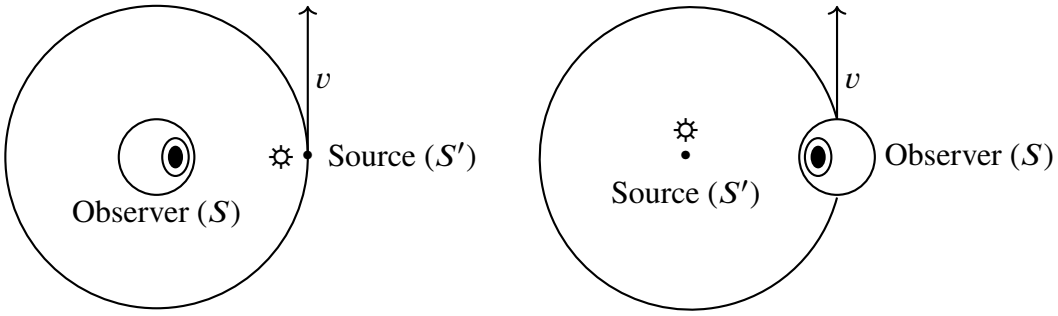

Figure 10: Two examples of transverse motion: Transverse motion in S resulting in redshift (left) and transverse motion in S' resulting in blueshift (right).

3.2.2 Transverse Doppler Effect

With transverse motion, it is necessary to take into account the influence of aberration: The meaning of the direction of movement being at right angles to the vector between the observer and the source is dependent on the frame. Superficial analysis not taking aberration into account might suggest that a planet orbiting a star a perfectly circular orbit would experience Doppler redshift but in fact it will experience blueshift.

Substitution of $\theta = \pi/2$ to (117) yields expression for transverse motion in S

$$\omega = \frac{\omega'}{\gamma} < \omega' \tag{120}$$

However, substitution of $\theta' = \pi/2$ yields $\beta = \cos\theta$ and an expression for transverse motion in S'

$$\omega = \frac{\omega'}{\gamma(1-\beta^2)} = \gamma\omega' > \omega'. \tag{121}$$

That is, transverse motion from the viewpoint of the observer leads to a redshift and transverse motion from the viewpoint of the source leads to a blueshift. A planet orbiting a star on a circular orbit will experience Doppler blueshift of the starlight and a imaging satellite orbiting a planet will experience (Doppler) redshift (see Figure 10).

3.2.3 Boundary Between Redshift and Blueshift

As shown previously, maximum blueshift and redshift are obtained at angles $\theta = 0°$ and $\theta = 180°$, respectively. The boundary w.r.t. values θ between redshift and blueshift occurs when $\omega = \omega'$ or equivalently

$$\gamma(1-\beta\cos\theta) = 1 \quad \Leftrightarrow \quad \cos\theta = \frac{1}{\beta}\left(1 - \frac{1}{\gamma}\right). \tag{122}$$

The limit is depicted in Figure 11. When β becomes larger, the region of blueshift gets smaller and converges to a dot when $\beta \to 1$.

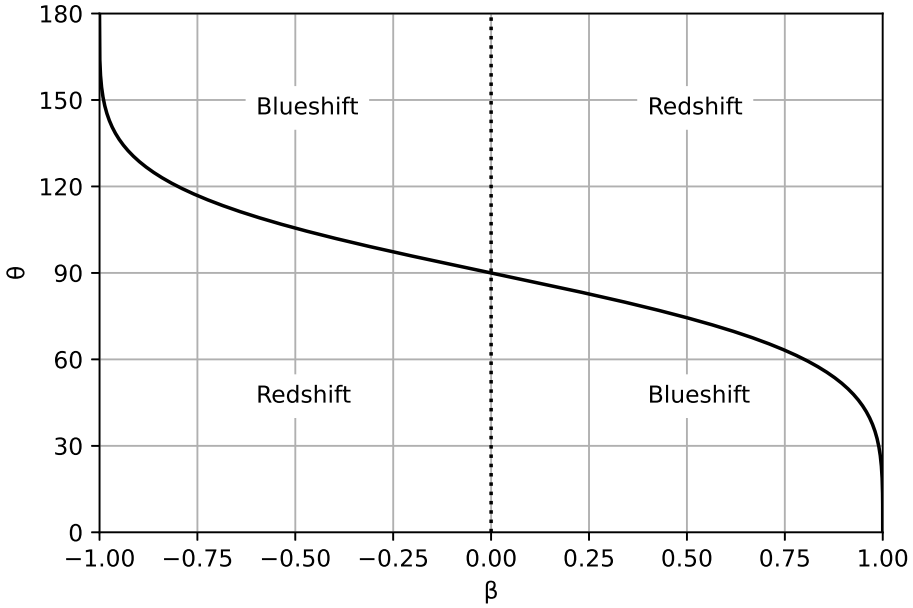

Figure 11: Limit angle between redshift and blueshift. For positive and negative β, the value is the lower and upper limit, respectively of the blueshift for θ.

4 Perception and Spectrum

4.1 Visual Perception

4.1.1 Human Vision and LMS Color Space

Human vision is limited to the wavelength range between 380 and 700 nm. The perception of color is based on three classes of cone cells on the retina. Each type of cone cell has different **spectral sensitivity**. That is, they are sensitive to different ranges of wavelengths. We can refer to the three classes according to their peak wavelength as long (L), medium (M) and short (S) with peaks at 560, 530 and 420 nm, respectively.

Let $S(\lambda)$ be the **spectral power distribution** ($\mathrm{W/m^2/nm}$) of the light received by the eye. If $\overline{L}(\lambda)$, $\overline{M}(\lambda)$, $\overline{S}(\lambda)$ are cone response functions

$$L = \int_0^\infty S(\lambda)\overline{L}(\lambda)\, d\lambda \tag{123}$$

$$M = \int_0^\infty S(\lambda)\overline{M}(\lambda)\, d\lambda \tag{124}$$

$$S = \int_0^\infty S(\lambda)\overline{S}(\lambda)\, d\lambda, \tag{125}$$

they are called **Color Matching Functions (CMFs)** for the **LMS Color Space**. The cone response functions are normalized so that their maxima are equal to unity (see Figure 12). The triplets

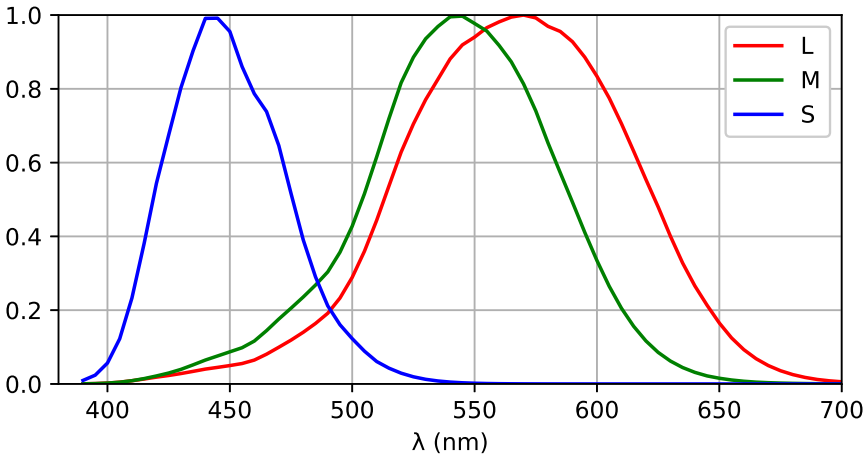

Figure 12: LMS color-matching functions $\overline{L}(\lambda), \overline{M}(\lambda), \overline{S}(\lambda)$.

(L, M, S) obtained above are called the **tristimulus values**. Two different spectra resulting in the same tristimulus values are called **metamers**.

4.1.2 CIE 1931 Color Spaces and sRGB Encoding

We wish to convert spectrum to 8-bit sRGB values that can be rendered on computer displays. This can be achieved by the use of CIE XYZ color-matching functions and then performing a conversion to SRGB and subsequent quantization. The XYZ color-matching functions are shown in Figure 13 and the corresponding tristimulus values are obtained via the inner products

$$X = \int_0^\infty S(\lambda)\overline{X}(\lambda)\, d\lambda \tag{126}$$

$$Y = \int_0^\infty S(\lambda)\overline{Y}(\lambda)\, d\lambda \tag{127}$$

$$Z = \int_0^\infty S(\lambda)\overline{Z}(\lambda)\, d\lambda. \tag{128}$$

Then, linear sRGB values between in the interval $[0, 1]$ can be obtained via the matrix product

$$\begin{bmatrix} R_{sRGB} \\ G_{sRGB} \\ B_{sRGB} \end{bmatrix} = \begin{bmatrix} 3.2406255 & -1.5372080 & -0.4986286 \\ -0.9689307 & 1.8757561 & 0.0415175 \\ 0.0557101 & -0.2040211 & 1.0569959 \end{bmatrix} \begin{bmatrix} X \\ Y \\ Z \end{bmatrix} \tag{129}$$

and clipping values below 0 and above 1 to 0 and 1, respectively. Before quantization, a "gamma" transfer function is applied

$$C'_{sRGB} = \begin{cases} 12.92\, C_{sRGB}, & C_{sRGB} \leq 0.0031308 \\ 1.055(C_{sRGB})^{(1/2.4)} - 0.055, & C_{sRGB} > 0.0031308 \end{cases} \tag{130}$$

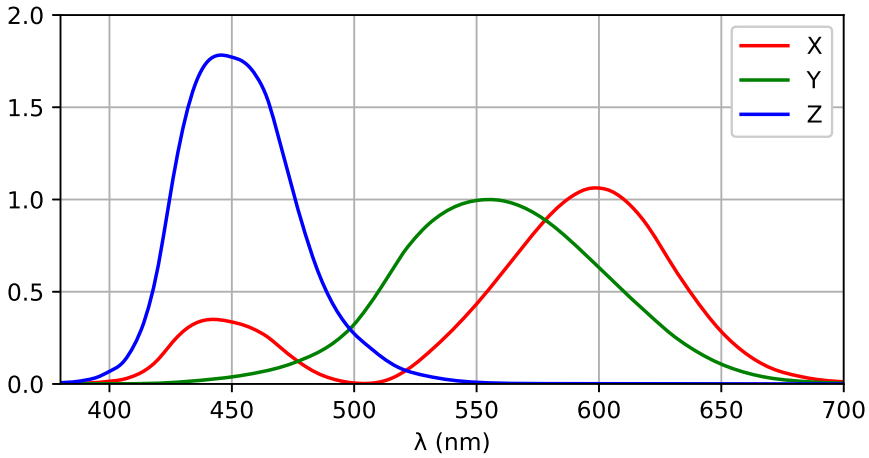

Figure 13: The CIE XYZ color-matching functions $\overline{X}(\lambda), \overline{Y}(\lambda), \overline{Z}(\lambda)$.

where $C \in \{R, G, B\}$. Finally, the 8-bit quantized values are obtained via

$$\begin{bmatrix} R_{sRGB(8)} \\ G_{sRGB(8)} \\ B_{sRGB(8)} \end{bmatrix} = \text{round}\left(255 \begin{bmatrix} R'_{sRGB} \\ G'_{sRGB} \\ B'_{sRGB} \end{bmatrix}\right) \tag{131}$$

4.1.3 Example: Visible Wavelength Range

To compute sRGB values corresponding to the visible wavelength range, select for each wavelength λ'

$$S(\lambda) := \frac{1}{2}\delta(\lambda - \lambda'), \tag{132}$$

where δ is the Dirac delta function. The factor is used to avoid saturation in cases where the linear sRGB values become larger than 1. Then,

$$X = \frac{1}{2}\int_0^\infty \delta(\lambda - \lambda')\overline{X}(\lambda)\, d\lambda = \frac{1}{2}\overline{X}(\lambda'), \tag{133}$$

$$Y = \frac{1}{2}\int_0^\infty \delta(\lambda - \lambda')\overline{Y}(\lambda)\, d\lambda = \frac{1}{2}\overline{Y}(\lambda'), \tag{134}$$

$$Z = \frac{1}{2}\int_0^\infty \delta(\lambda - \lambda')\overline{Z}(\lambda)\, d\lambda = \frac{1}{2}\overline{Z}(\lambda'), \tag{135}$$

and application of (129) and (130) yield Figure 14.

4.2 Basic Radiometry

4.2.1 Black-Body Radiance

Luminosity (also called **radiant flux**) L (W) for a closed surface is an absolute measure of radiated electromagnetic energy per unit time. The luminosity of Sun is denoted $L_\odot$. **Radiance** for a source

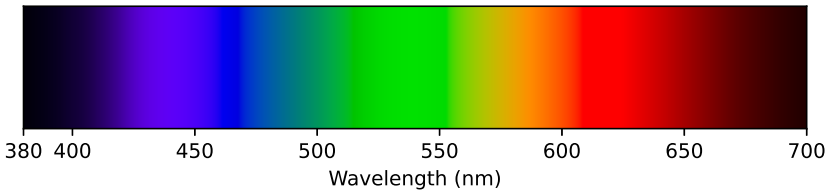

Figure 14: RGB values obtained with (132).

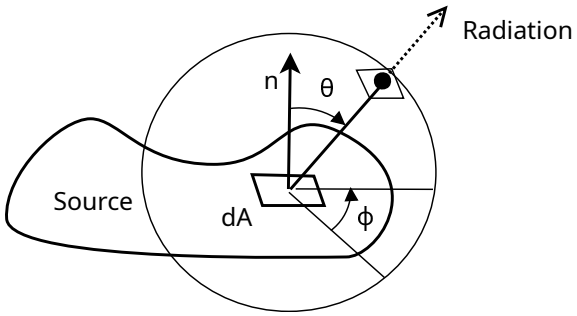

Figure 15: Geometry associated to the definition of radiance.

L_e is the radiant flux from a given surface per unit projected area. That is,

$$L_e = \frac{\partial}{\partial \Omega} \frac{\partial L}{\partial A \cos\theta} \tag{136}$$

where Ω is the solid angle around the surface element dA, A is the area on the source and $\theta \in [0, \pi/2]$ is the angle between the surface normal and the point on the unit sphere (see Figure 15). Projection of an area element dA to the direction θ w.r.t. surface normal is equal to $\cos\theta\, dA$.

Spectral radiance in frequency or wavelength are defined

$$L_{e,\nu} := \frac{\partial L_e}{\partial \nu} \quad \Leftrightarrow \quad L_e = \int_0^\infty L_{r,\nu}(\nu)\, d\nu \tag{137}$$

$$L_{e,\lambda} := \frac{\partial L_e}{\partial \lambda} \quad \Leftrightarrow \quad L_e = \int_0^\infty L_{r,\lambda}(\lambda)\, d\lambda, \tag{138}$$

respectively. Spectral radiance of a **black-body** can be written

$$L_{e,\nu}(\nu) = \frac{2h\nu^3}{c^2} \left[\exp\left(\frac{h\nu}{kT}\right) - 1 \right]^{-1} \tag{139}$$

$$L_{e,\lambda}(\lambda) = \frac{2hc^2}{\lambda^5} \left[\exp\left(\frac{hc}{\lambda kT}\right) - 1 \right]^{-1}, \tag{140}$$

where $h = 6.62607015 \cdot 10^{-34}\ \mathrm{J \cdot Hz^{-1}}$ is the **Planck's constant** and $k = 1.380649 \cdot 10^{-23}\ \mathrm{J \cdot K^{-1}}$ is

the **Bolzmann constant**. To obtain radiance, we integrate over all frequencies

$$L_e = \frac{2h}{c^2} \int_0^\infty \frac{\nu^3 \, d\nu}{\exp\left(\frac{h\nu}{kT}\right) - 1} \tag{141}$$

using the substitution $x = h\nu/kT$. Substituting correspondingly $\nu = kT/h \, x$ and $d\nu = kT/h \, dx$, we obtain

$$L_e = \frac{2h}{c^2} \left(\frac{kT}{h}\right)^4 \int_0^\infty \frac{x^3 \, dx}{e^x - 1} = \frac{2h}{c^2} \left(\frac{kT}{h}\right)^4 \Gamma(4)\zeta(4), \tag{142}$$

where Γ and ζ are the Gamma and Riemann zeta functions. Substitution of $\Gamma(4) = 6$ and $\zeta(4) = \pi^4/15$ yields

$$L_e = \frac{2 \, k^4 \pi^4}{15 \, h^3 c^2} \, T^4. \tag{143}$$

To obtain the radiant flux, we integrate the radiance over a hemisphere of solid angles and the entire surface

$$L = \oint_A \int_\Omega L_e(\boldsymbol{r}, \theta, \phi) \cos\theta \, d\Omega \, dA \tag{144}$$

where $\boldsymbol{r}$ is a point on the surface element dA. The computation of the integral is simplified by the intependence of radiance (143) from θ and ϕ. For solid angle, we can expand $d\Omega = \sin\theta \, d\theta d\phi$. Thus,

$$L = \oint_A L_e \int_0^{2\pi} \int_0^{\pi/2} \sin\theta \cos\theta \, d\theta \, d\phi \, dA = \pi \oint_A L_e \, dA. \tag{145}$$

If L_e is independent of position on the surface (e.g. due to equal temperature), we obtain

$$L = \pi A L_e. \tag{146}$$

For a black-body, this yields the **Stefan-Boltzmann law**

$$L = \pi A L_e = \frac{2}{15} \frac{k^4 \pi^5}{h^3 c^2} A T^4 = \sigma A T^4, \tag{147}$$

where the **Stefan-Boltzmann constant**

$$\sigma = \frac{2k^4 \pi^5}{15 h^3 c^2} = 5.670374419 \cdot 10^{-8} \, \mathrm{W} \cdot \mathrm{m}^{-2} \cdot \mathrm{K}^{-4}. \tag{148}$$

4.2.2 Wien's Displacement Law

To obtain peak frequency of the black body radiance as a function of temperature, we derivate (139) w.r.t. frequency

$$\frac{\partial L_{e,\nu}}{\partial \nu} = \frac{6h\nu^2}{c^2} \left[\exp\left(\frac{h\nu}{kT}\right) - 1\right]^{-1} - \frac{2h^2\nu^3}{c^2 kT} \exp\left(\frac{h\nu}{kT}\right) \left[\exp\left(\frac{h\nu}{kT}\right) - 1\right]^{-2} = 0. \tag{149}$$

Substitution of $x = h\nu/kT$ yields

$$x = 3(1 - e^{-x}), \tag{150}$$

which admits numerical solution

$$x = \frac{h\nu}{kT} \approx 2.821439372122078893 \tag{151}$$

Thus, the black-body radiance obtains it's peak at the frequency

$$\nu_{peak} = \frac{kT}{h} x \approx 5.878925757646824946T \cdot 10^{10}\,\mathrm{Hz} \cdot \mathrm{K}^{-1} \tag{152}$$

To obtain peak wavelength of the black body radiance as a function of temperature, we derivate (140) w.r.t. wavelength

$$\frac{\partial L_{e,\lambda}}{\partial \lambda} = -\frac{10hc^2}{\lambda^6}\left[\exp\left(\frac{hc}{\lambda kT}\right) - 1\right]^{-1} + \frac{2h^2c^3}{\lambda^7 kT}\exp\left(\frac{hc}{\lambda kT}\right)\left[\exp\left(\frac{hc}{\lambda kT}\right) - 1\right]^{-2} = 0. \tag{153}$$

Substitution of $y = hc/\lambda kT$ yields

$$y = 5(1 - e^{-y}), \tag{154}$$

which admits numerical solution

$$y = \frac{hc}{\lambda kT} \approx 4.965114231744276303. \tag{155}$$

Thus, the black-body radiance obtains it's peak at the wavelength

$$\lambda_{peak} = \frac{hc}{ky}\frac{1}{T} \approx 2.897771955/T \cdot 10^{-3}\,\mathrm{m} \cdot \mathrm{K}. \tag{156}$$

The equation (156) is called the **Wien's displacement law** and is usually written in terms of the constant of proportionality $b = hc/ky$ called the **Wien's displacement constant**. Note that when the blackbody radiance is expressed as a function of wavelength and frequency, the peak occurs at a different frequency in the sense that we cannot transform between the peak wavelength and peak frequency with the relation $\lambda\nu = c$.

Three examples of black-body spectra are shown in Figure 16. Substitution of $T = 4000\mathrm{K}, 5000\mathrm{K}$ and $6000\,\mathrm{K}$ yields $\lambda_{max} = 724.44\,\mathrm{nm}, 579.55\,\mathrm{nm}$ and $482.96\,\mathrm{nm}$, respectively. The increasing spectral radiance of the curves seems consistent with (147) since $5^4/4^4 \approx 2.44$ and $6^4/5^4 \approx 2.49$.

4.2.3 Effective Temperature and Color

Visual perception of black-body as a function of its **effective temperature** is easily obtained using the computation in section 4.1.2. In Figure 17, SRGB values for black-bodies are displayed for a temperature range. The XYZ-values have been normalized before SRGB conversion by division with $\max\{X, Y, Z\}$.

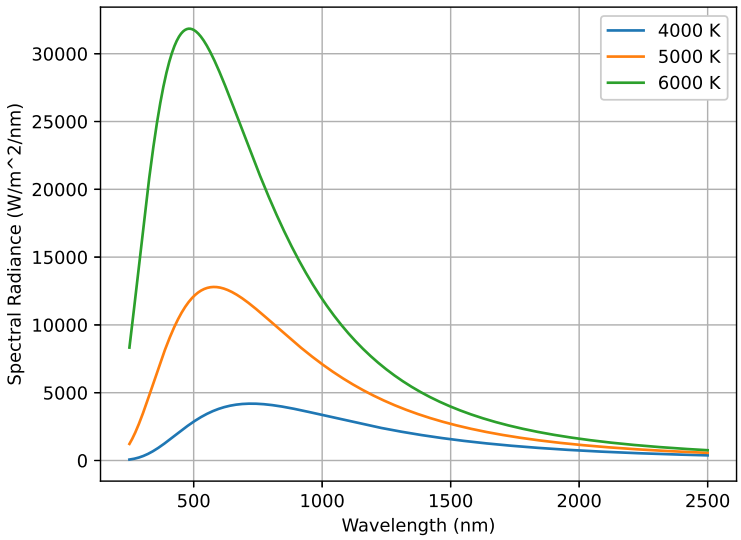

Figure 16: Three examples of black-body spectra.

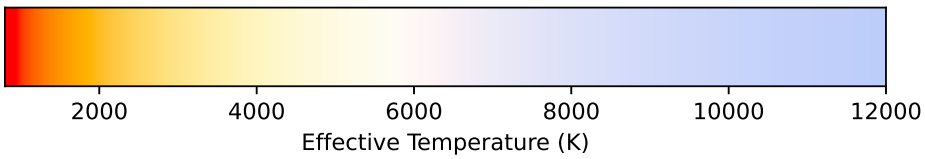

Figure 17: Visual perception of color for black-bodies at temperatures between 800 K and 12000 K.

4.2.4 Doppler Transformation and Black-Body Radiance

For an observer moving at relativistic speeds, the perceived color of black-body sources can be significantly influenced by the Doppler effect. However, since the black-body radiation is not monochromatic but consists of a continuous spectrum, the computation of the Doppler effect is no longer trivial.

4.3 Stars

4.3.1 Spectral Classification of Stars

4.3.2 Observed Spectral Power Distribution

4.3.3 Doppler Effect

4.4 Planets

5 Visual Effects at Relativistic Speeds

5.1 Deformation

5.1.1 Grid Deformation

5.1.2 Solid Objects

5.2 Brightness

5.2.1 Headlight Effect